SUPPLEMENTAL MATERIAL

Supplemental Methods

Human adipose-derived stem cell (ADSC) isolation and culture

Human ADSCs were isolated using a modified protocol, as described previously.[1] Human abdominal subcutaneous adipose tissues were obtained from 19 healthy adults (20-30 year-old, female) during liposuction. The tissue was obtained per a tissue acquisition protocol approved by the Medical Ethics Committee of the Third Military Medical University (Permit Number: 2012[13]). All the tissue donors involved were provided written informed consent, and the consent procedure was developed and approved by the Medical Ethics Committee. Adipose tissue was minced and incubated for 45 minutes at 37°C on a shaker with 0.1% collagenase I (Worthington) in a phosphate-buffered saline (PBS) with 2 mM calcium chloride. The digested tissue was sequentially filtered through 100-μm and 40-μm filters (BD) and centrifuged at 300 g for 5 minutes at room temperature. The supernatant containing adipocytes and debris was discarded.

ADSCs were suspended in Dulbecco's modified eagle medium (DMEM)/Ham's F-12 (Gibco) containing 10% fetal bovine serum (FBS), 2 mM glutamine, 100 U/ml penicillin, and 100 μg/ml streptomycin and cultured at 37°C in a humidified atmosphere containing 5% CO_2. Cultures were washed daily to remove unattached cells. Plastic-adherent cells were referred to as ADSCs. After the ADSCs reached confluence, they were reseeded at a density of 3,000 cells/cm^2. ADSCs of passage 3 were used for experiments, which were demonstrated to be with ASDC surface markers ($CD90^+$, $CD73^+$, $CD44^+$, $CD105^+$, $CD34^-$ and $CD45^-$) and multi-lineage differentiation potential (lipogenesis and osteogenesis), similar to those previously reported.[1] For *in vitro* studies, administration of 200 μM H_2O_2 for 6 hours was used to induce oxidative injury.

Lentiviral shPHD2 transduction of ADSCs

The human PHD2 (Gene Bank ID: NM_022051) small hairpin RNA (shRNA) was constructed into the lentivirus gene transfer vector pGC SIL-green fluorescent protein (GFP) from Genechem Co., Ltd. (Shanghai, China). To minimize the risk that the phenotype is an off-target effect, four shRNA clones against PHD2 and an irrelevant sequence were tested. Both lentiviruses containing GFP or shPHD2-GFP were used with a MOI of 10:1. An infection cocktail containing lentiviral supernatant, 5 mg/mL polybrene, and 10% FBS in DMEM/F-12 with 2.5×10^5 was added to ADSCs cultured in 60 mm dishes for 24 hours at 37°C with 5% CO_2. The medium was removed and replaced with fresh medium and ADSCs were incubated for another 24 hours. Successful lentiviral transduction was determined by detecting GFP fluorescence and PHD2 protein expression. Transfected ADSCs were enriched by fluorescence-activated cell sorting with FACSAria II (BD Biosciences). Human HIF-1α shRNA lentiviral particles (and control shRNA lentiviral particles) were purchased from Santa Cruz Biotechnology. The infection protocol of HIF-1α shRNA lentiviral particles was similar to that of lentiviral PHD2 shRNA.

Cardiomyocyte isolation and culture

Primary cultures of neonatal rat ventricular myocytes (NRVMs) from 1-2-day-old Sprague-Dawley rat pups were prepared using the method described in detail previously.[2, 3] Immediately after euthanasia of rat pups, hearts were removed, ventricles were minced, and myocytes were dissociated with trypsin (1.5 mg/mL, Difco). Dissociated cells were then collected at 10-min intervals. The cells were re-suspended in DMEM (Gibco) supplemented with 5% FBS and 0.1 mM BrdU, and plated in culture dishes for 60 minutes to allow fast-adherent fibroblasts to attach. Non-adherent cells (ventricular myocytes) were collected and plated in other culture dishes or coverslips coated with fibronectin at a density of 160 cells/mm^2. On the following day, the medium was replaced with DMEM containing 5% FBS (Hyclone) but without BrdU. For *in vitro* studies, administration of 100 μM H_2O_2 for 6 hours was used to induce oxidative injury.

Experiments using the animals were conducted with the approval of the Animal Care and Use

Downloaded from http://circres.ahajournals.org/ at Temple University--Philadelphia on June 11, 2013

Committee of Third Military Medical University (Approval ID: SCXK (Military) 2007015), according to the State Science and Technology Commission Regulations for the Administration of Affairs Concerning Experimental Animals (1988, China). All surgeries were performed under isoflurane anesthesia, and all efforts were made to minimize animal suffering.

Mouse myocardial infarction (MI) and intramyocardial cell delivery

Permanent ligation of left anterior descending (LAD) coronary artery and cell injection were performed in male C57 mice (8 weeks old) as described previously.[4] Anesthesia was maintained with isoflurane inhalation. A permanent ligation was performed around the LAD coronary artery 2-3 mm from its origin with a 7-0 silk suture. Sham-operated animals were subjected to the same surgical procedures except that the suture was passed under the LAD but not tied.

Immediately after MI injury, 1×10^5 donor ADSCs suspended in 50 μL PBS were injected at 5 sites (10 μL per each site) in the anterior and posterior infarct border zones of the ischemic myocardium.

Human ADSCs have a low immunogenic profile and do not elicit significant inflammatory response and survived for a long time in rabbits and mice.[5, 6] Furthermore, to enhance the immune suppression, FK506 (3mg/kg/day, i.p., Sigma) was administered to ADSC-transplanted and sham-operated animals daily from 1 week before the operation and for the whole duration of the study, similar to previous studies.[7] Animal care and all experimental procedures were performed in strict accordance with the approved protocols and animal welfare regulations of the Animal Care and Use Committee at Third Military Medical University.

Area at risk (AAR) and infarct size determination

AAR was defined by Evans blue dye, and the infarct size was defined by triphenyltetrazolium chloride (TTC) straining. Briefly, 0.3 ml of 1.5% Evans blue in PBS was injected retrograde into the brachiocephalic artery. The non-ischemic area, which was not at risk, was stained blue. The heart was excised and cut into five 1-mm-thick transverse slices, parallel to the atrioventricular groove. AAR was calculated by dividing the total non-blue area by the total area of the left ventricle (LV) sections. Each slice was incubated in a 1% solution of TTC at 37°C for 15 minutes to differentiate infarct area (pale) from viable (brick red) myocardial area. For hearts subjected to MI for more than 2 weeks, the ratio of the length of the infarct band to the total length of the LV was calculated and expressed as a percentage. The AAR and infarct area from each section were measured using Image J software, and the values obtained were averaged. Individuals conducting the experiment were blinded to the experimental groups.[8]

Echocardiography analysis

Echocardiography was performed (GE vivid 7 dimension) to determine cardiac structure and function in conscious mice.[9, 10] Hearts were viewed in the short-axis between the two papillary muscles and each measurement was obtained with M-mode by averaging results from three consecutive heart beats. Fractional shortening (%FS) was calculated as follows: $\%FS = (LVIDd - LVIDs)/LVIDd \times 100$, where LVIDd is diastolic LV internal diameter and LVIDs is systolic LV internal diameter. Left ventricular ejection fraction (EF) was automatically calculated by the echocardiography software according to the Teicholz formula. Parameters including LVIDd were measured to determine structural changes in cardiac morphology. The individuals conducting the experiment were blinded to the animal treatments.

Tissue section histopathology

Formalin fixed hearts were processed, embedded in paraffin and cut as 5 μm-thick sections. To track the phenotypes of GFP^+ ADSCs in hearts, anti-GFP antibody (Invitrogen), anti-von Willebrand factor (vWF) antibody (Santa Cruz), anti-smooth muscle actin (SMA) antibody (Santa Cruz), anti-sarcomeric tropomyosin antibody (Sigma) and anti-sarcomeric α-actinin (Sigma) were used. To detect capillary density in peri-infarct myocardium, a rat anti-mouse CD31 was used.[11] To detect cardiomyocyte apoptosis, an in situ apoptotic cell death detection kit (POD; Roche Applied Bio Sciences) based on the

Downloaded from http://circres.ahajournals.org/ at Temple University--Philadelphia on June 11, 2013

TUNEL assay was used.[8] The percentage of apoptotic nuclei per section was calculated by counting the number of TUNEL-staining cardiomyocyte nuclei divided by the total number of DAPI-positive nuclei. Cardiomyocyte cytoplasm was identified by sarcomeric tropomyosin antibody. The number of capillaries and apoptosis was counted in 5 randomly fields per section of the peri-infarct zone, and a total of 5 sections per animal were analyzed (N=5 for each group). As reported in our previous studies,[12] cardiac fibrosis was quantitated by measuring the blue area in the Masson's trichrome-stained heart sections. Alexa Fluor 488 or Alexa Fluor 647-conjugated secondary antibodies (Jackson ImmunoResearch) were applied appropriately. DAPI was used for nuclear counterstaining. Images were taken at a magnification of 20× with a Nikon fluorescence microscope (Tokyo, Japan). All the manual counts were performed in a blinded fashion.

Immunocytofluorescence analysis of NF-κB

Briefly, ADSCs were cultured on coverslips. Culture medium was removed, and cells were fixed in 4% paraformaldehyde for 20 min at room temperature. Fixed cells were incubated with blocking buffer containing 3% BSA for 30 min, treated with anti-NF-κB p65 antibody (1:100, Santa Cruz) overnight at 4°C, and then with an Alexa Fluor 647-conjugated secondary antibody for 60 min at room temperature. Images were taken with a Nikon fluorescence microscope (Tokyo, Japan). The manual counting was performed in a blinded fashion. BAY11-7082（Sigma, 5 μM）and dominant negative IκBα plasmid (generous gift from Dr. Rongtuan Lin of McGill University in Canada)[13] was used for inhibition of NF-κB activation.

Western blotting

ADSC lysates with equal total protein amount were separated by SDS-PAGE gel. Proteins were transferred electrophoretically to PVDF membranes (Bio-Rad). The membranes were blocked in 5% milk in PBS-T (0.1% Tween20) at room temperature for 1 hour. Then membranes were probed with primary antibody specific for PHD1 (1:500; Abcam), PHD2 (1:500; Novus Biologicals), PHD3 (1:500; Abcam), activated (cleaved) caspase-3 (1:200; Abcam), total caspase-3 (1:200; Abcam), HIF-1α (1:500; Santa Cruz), phospho-IKKβ (1:200; Santa Cruz), total IKKα (1:500; Santa Cruz), total IKKβ (1:500; Santa Cruz), phospho-IκBα (1:200; Santa Cruz) and total IκBα (1:500; Santa Cruz). The primary antibody was then identified by an HRP-conjugated secondary antibody diluted 1:5000 (Cell signaling technology). Finally, the membranes were developed using an ECL advance detection kit (GE healthcare) and exposed to X-ray films. The band density was analyzed using Quantity One software. The densitometric values were normalized with β-actin protein signal. Each analysis was done at least 3 times.

Quantitative PCR (qPCR)

Total RNA was extracted from cells with TRIzol (Invitrogen) and purified with RNeasy kits (Qiagen, Hilden, Germany). After reverse transcription (Superscript II, Invitrogen), qPCR was performed using the Brilliant SYBR Green Mastermix-Kit and the MX4000 multiplex qPCR System from Stratagene. PCR primers are: GLUT-1: Forward： 5’ tcactgtgctcctggttctg 3’; Reverse: 5’ cctcgggtgtcttgtcactt 3’. EPO: Forward：5’ tcatctgtgacagccgagtc 3’; Reverse: 5’ tttggtgtctgggacagtga 3’. IGF-1: Forward：5’ cccaacccagcccttattat 3’; Reverse: 5’ ccccatctcacaaaaaggaa 3’.

Chromatin immunoprecipitation (ChIP) assay

Three NF-κB binding sites in IGF-1 promoter were predicted using TFSEARCH (www.cbrc.jp/research/db/TFSEARCH.html). ChIP assay for the IGF-1 promoter region was performed using the EZ-ChIP kit (millipore) according to the manufacturer’s instruction. Briefly, ADSCs pre-treated with NF-κB stimulator LPS (1μg/ml for 30min) were prepared and cross-linked with 1% formaldehyde for 10 min at room temperature. To shear the chromatin, the whole cell extract was sonicated after being resuspended in 0.45 ml lysis buffer. For IP, anti-NF-κB p65 (abcam) and anti-NF-κB p50 (abcam) were used. IP and Input DNA were purified using columns provided in the EZ-ChIP kit and then amplified

Downloaded from http://circres.ahajournals.org/ at Temple University--Philadelphia on June 11, 2013

using a rTaq PCR mastermix kit. Primers for the specific IGF-1 promoter region containing the predicted NF-κB binding site is designed as follow: Primers for detecting the DNA containing NF-κB binding site (-197 to -188) of human IGF-1 gene: Forward: 5' gtaaaggtgtcctgcccaga 3'; Reverse: 5' ccactcccttactcccttcc 3'.

Antibody array

To prepare the conditioned medium (CM) of ADSCs, we used a modified method from that described previously.[14, 15] Different batches of ADSCs with or without shPHD2 (1×10^6 cells) were cultured in a serum-free medium in the absence of growth factors for 24 hours. CM was collected and then stored for use.

Human Cytokine Antibody Array C series 2000 membranes (Ray Biotech) targeting 79 secreted factors were incubated with 1 mL of conditioned ADSC supernatant for 2 hours, washed, and sequentially incubated with biotinylated antibodies, horseradish peroxidase-conjugated strepavidin, and detection solution according to the manufacturer's instructions.

ELISA analysis for cytokines and administration of neutralizing antibodies

The levels of VEGF, HGF, stromal cell-derived factor 1 (SDF-1), erythropoietin (EPO) and IGF-1 in the conditioned medium of ADSCs were determined by ELISA using commercially available Quantikine kits (R&D) according to the manufacturer's instruction. All samples and standards were measured in duplicates.

The 10:1 ratio of antibodies to cytokines was able to neutralize 90% of the released growth factor. IGF-1 neutralizing antibody (1:50, R&D) was added to the stem cell conditioned medium at final concentrations of 12 ng/mL and to the stem cells injected into post-MI hearts at the same concentration.

NF-κB activity ELISA

Similar to previous studies,[16, 17] activation of NF-κB p65 was determined by ELISA using a commercially available ELISA kit. Nuclear extracts of ADSCs were prepared with the NucBuster protein extraction kit (Novagen), and 5 μg of nuclear extract was used to determine the DNA binding of NF-κB subunit p65 with the TransAM NF-κB p65 kit (Active Motif), according to the manufacturer's protocol. In this assay, tissue lysates were tested for their abilities to bind to a double-stranded oligonucleotide probe containing the consensus binding sequence (5′-GGGACTTTCC-3′) of NF-κB. The active form of NF-κB in the nuclear extract specifically binds to this consensus site and is recognized by a primary antibody specific for the activated form of p65 of NF-κB. A horseradish peroxidase-conjugated secondary antibody provides the basis for the colorimetric quantification. The absorbance of the resulting solution was measured on a spectrophotometer within 5 min at 450 nm.[18] This method was used as an alternative to electrophoretic mobility shift assay (EMSA), since it has been reported to be more sensitive and quantitative.[19] The OD450 was read on a spectrophotometer (Thermo Scientific). All samples and standards were measured in duplicate.

[^{3}H]thymidine incorporation assay

The [^{3}H]thymidine incorporation experiments were performed using the method previously described[20] with modifications. Briefly, ADSCs were arrested in the G_0/G_1 phase by serum deprivation for 24 h. Cells were pulsed with 1 μCi [methyl-^{3}H]thymidine for 1 h at 37°C after incubation for 24, 48 or 72 hours, washed twice with PBS, fixed in 10% trichloroacetic acid (TCA) at 23°C for 15 min, and washed twice with ethanol. The acid-insoluble materials were dissolved in 2 N NaOH at 23°C for 12 h, and the levels of radioactivity were measured with a liquid scintillation counter (Beckman LS6500). Absolute counts were converted to a percentage of control (untreated) counts to facilitate comparisons between conditions.

Cell Counting Kit-8 (CCK-8) assay

As previously described,[21] the number of viable cells was assayed using CCK-8 kit (Dojindo) per

Downloaded from http://circres.ahajournals.org/ at Temple University--Philadelphia on June 11, 2013

the manufacturer's protocol. Briefly, ADSCs were plated into 96-well plate and incubated with CCK-8 for 2 hour at 37 °C. The absorbance was subsequently measured on a spectrophotometer (Thermo Scientific) at 450 nm. Three independent experiments were performed.

Fluorescence activated cell sorting (FACS) and flow cytometry analysis

To enrich the genetically modified ADSCs, the GFP^+ ADSCs were sorted with FACSAria II (BD Biosciences) three days after the lentiviral transduction. The purified GFP^+ ADSCs were then expanded in culture for use.

For live cell counting, hearts with MI were digested. Dissociated cells were separated by filtering through a 30μm filter. Most of the cardiomyocytes (>30 μm diameters) were discarded and the small cell fraction (<30 μm) was collected. The surviving GFP^+ cells were identified with fluorescence microscopy and the number of GFP^+ cells was counted with FACSAria II.

Combinations of antibodies including anti-CD90, CD73, CD44, CD105, CD34 and CD45 (1:200 each, BD Biosciences) were used to identify the characteristics of ADSCs. Anti-CD11b and Anti-Ly-6C (1:200 each, BD Biosciences) were used to analyze the inflammatory cell infiltration. Cells were subjected to flow cytometry on a BD FACS Calibur and data analyzed by FlowJo software.

For cell death detection, annexin V and propidium iodide (PI) double staining (Roche) and flow cytometry analysis were done. In brief, after treatment, ADSCs (1×10^6 cells/ml) were washed with PBS and resuspended in a binding buffer (10 mM HEPES/NaOH, pH 7.4, 140 mM NaCl, 2.5 mM $CaCl_2$). After incubated in the dark at room temperature for 20 minutes, the cell populations with Annexin-V/PI staining were analyzed with BD FACS Calibur.

Statistical Analysis

Data are reported as means±SEM. For analysis of differences between two groups, student's t test was performed. For multiple groups, ANOVA was carried out followed by Bonferroni post-hoc test. A P value of <0.05 was considered significant. In this study, n is the number of cells examined, and N is the animal number or times of cell cultures.

Downloaded from http://circres.ahajournals.org/ at Temple University--Philadelphia on June 11, 2013

Online Figure I

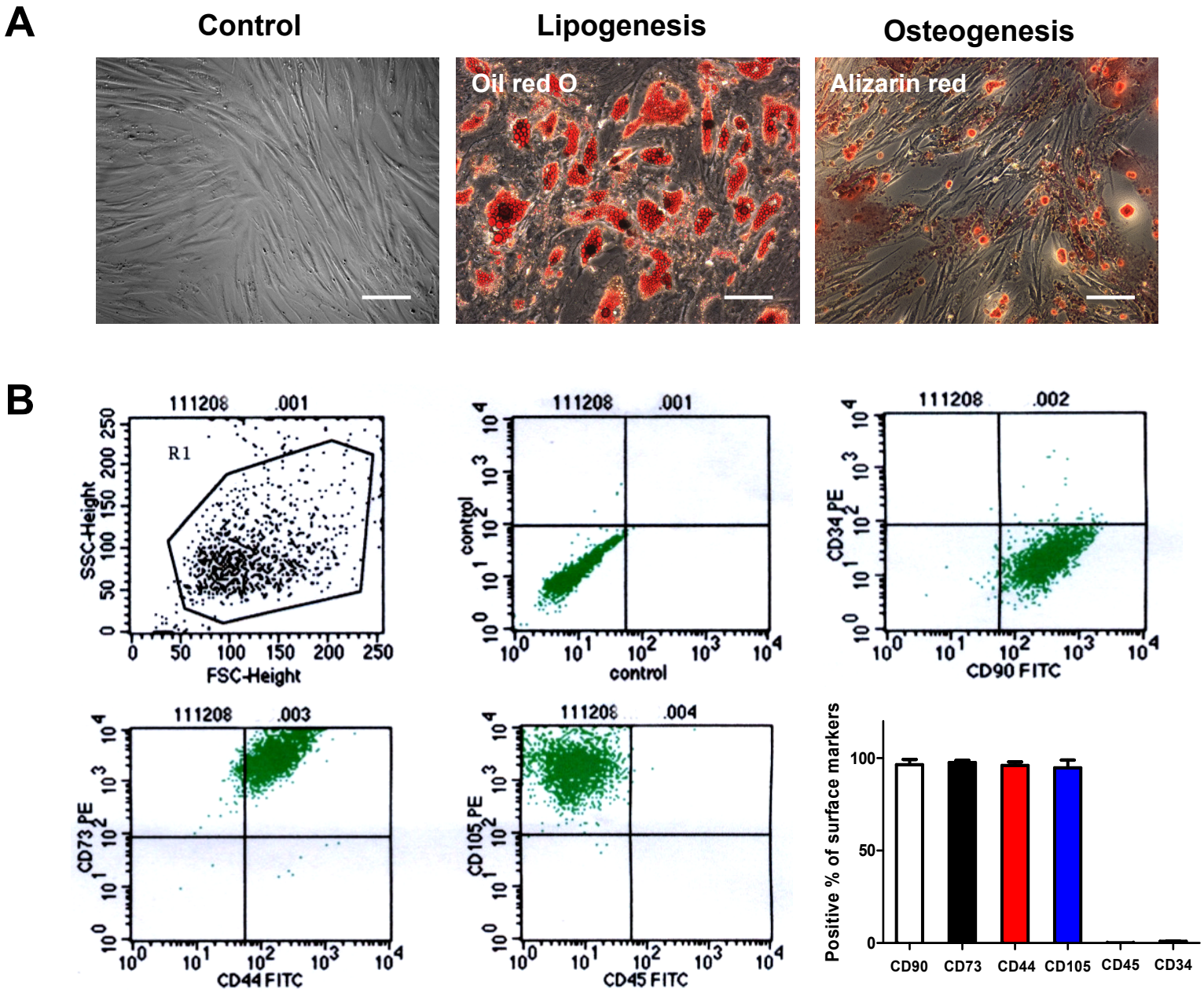

Online Figure II

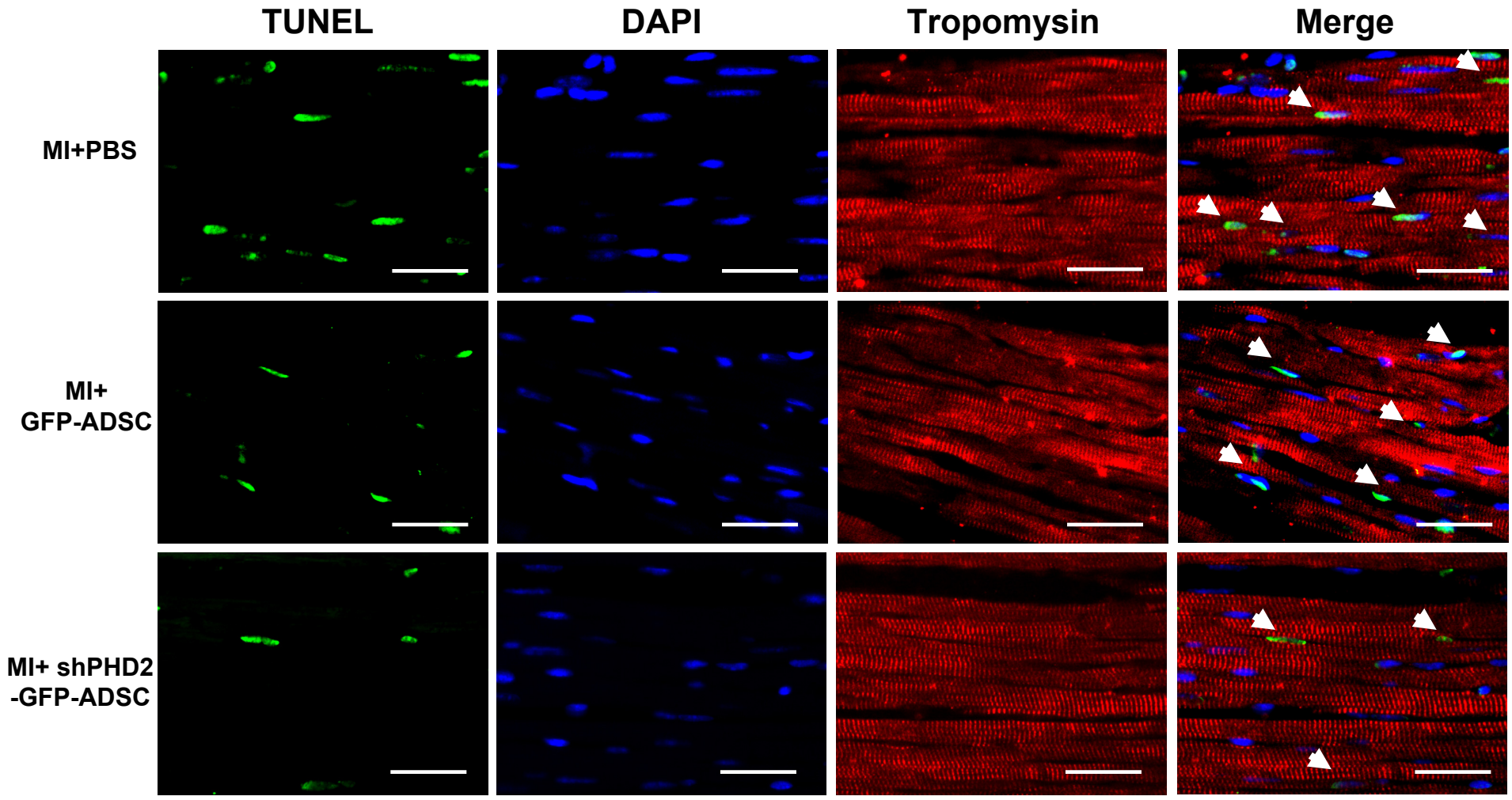

Online Figure III

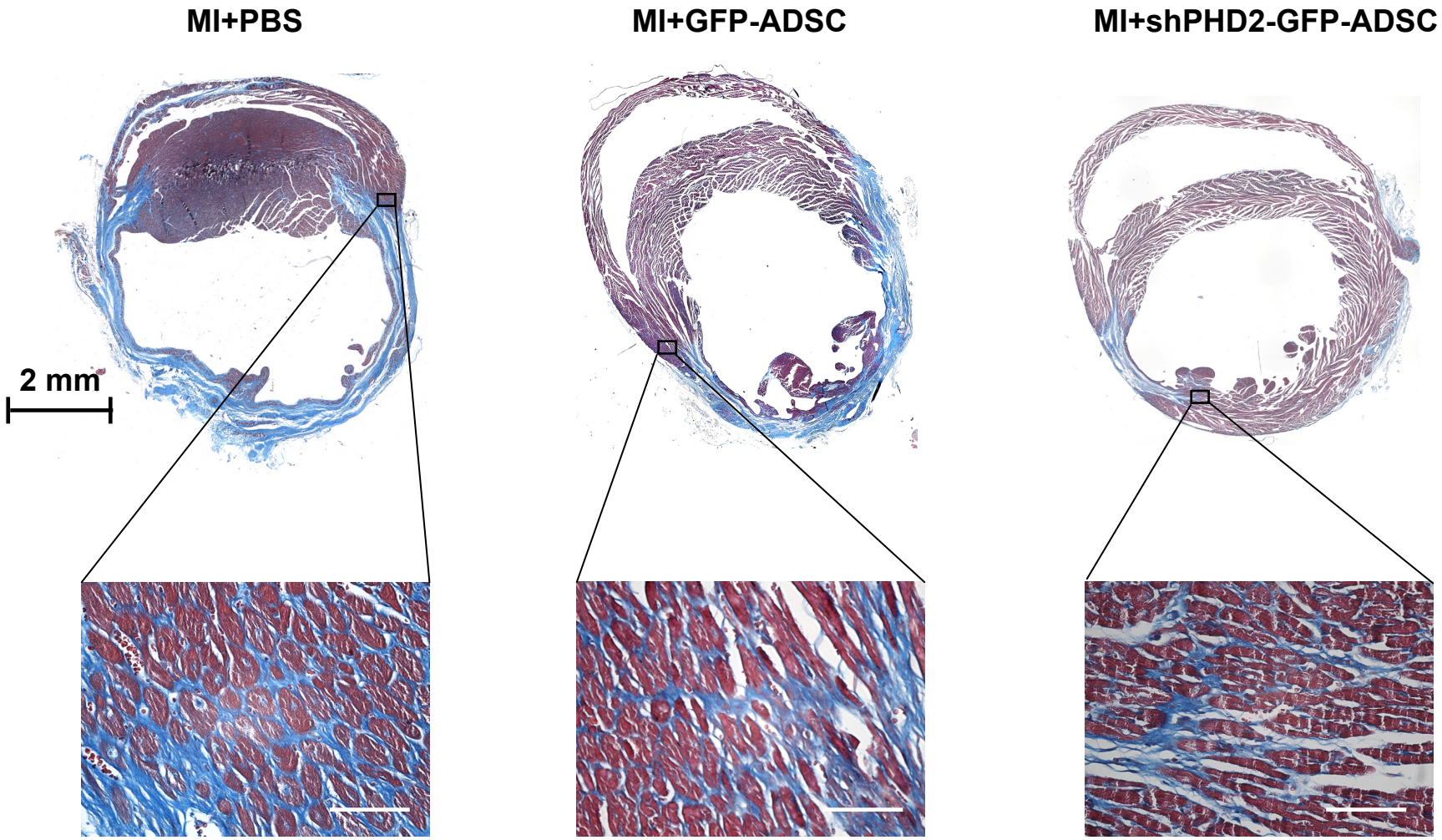

Online Figure IV

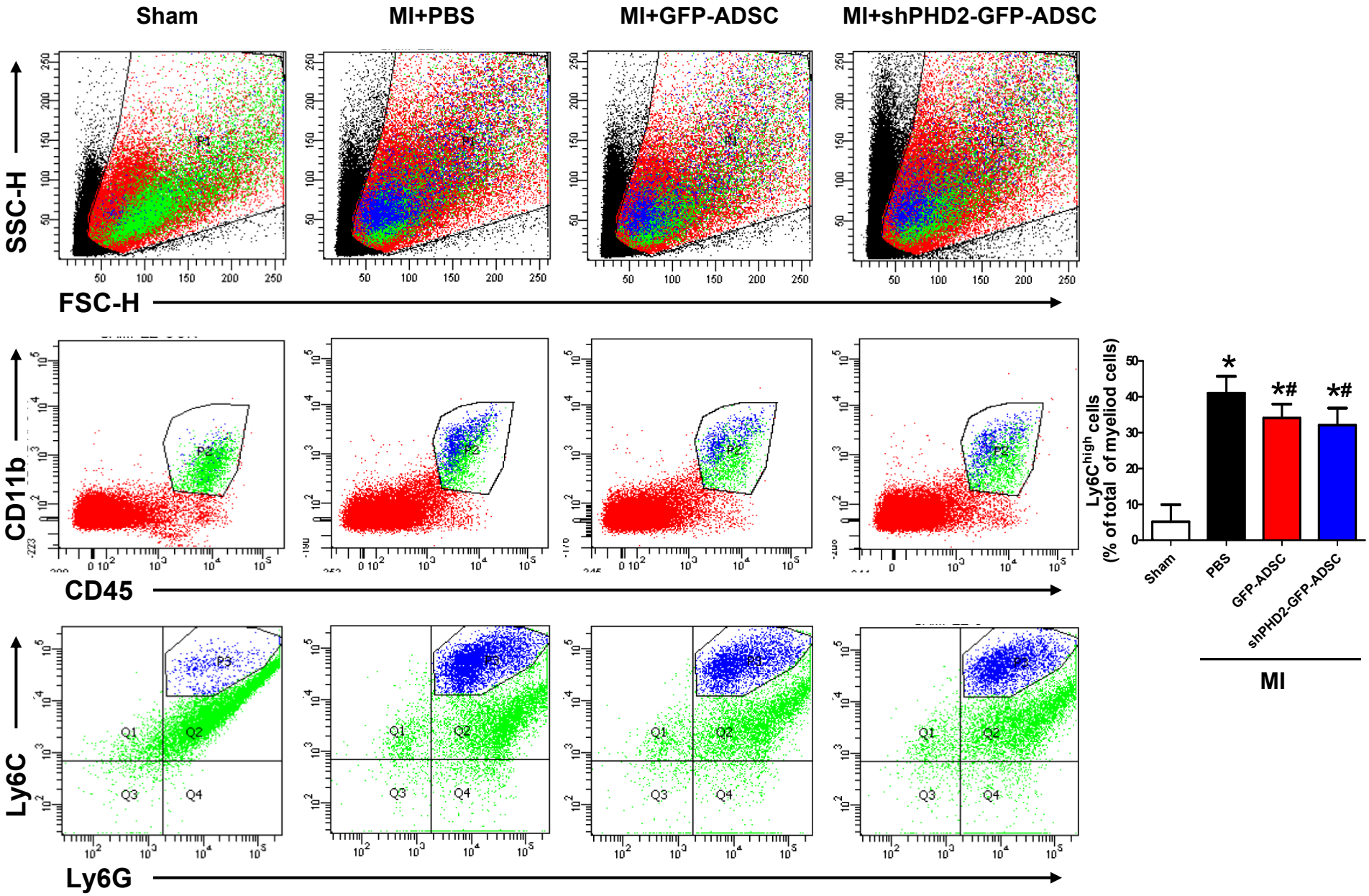

Online Figure V

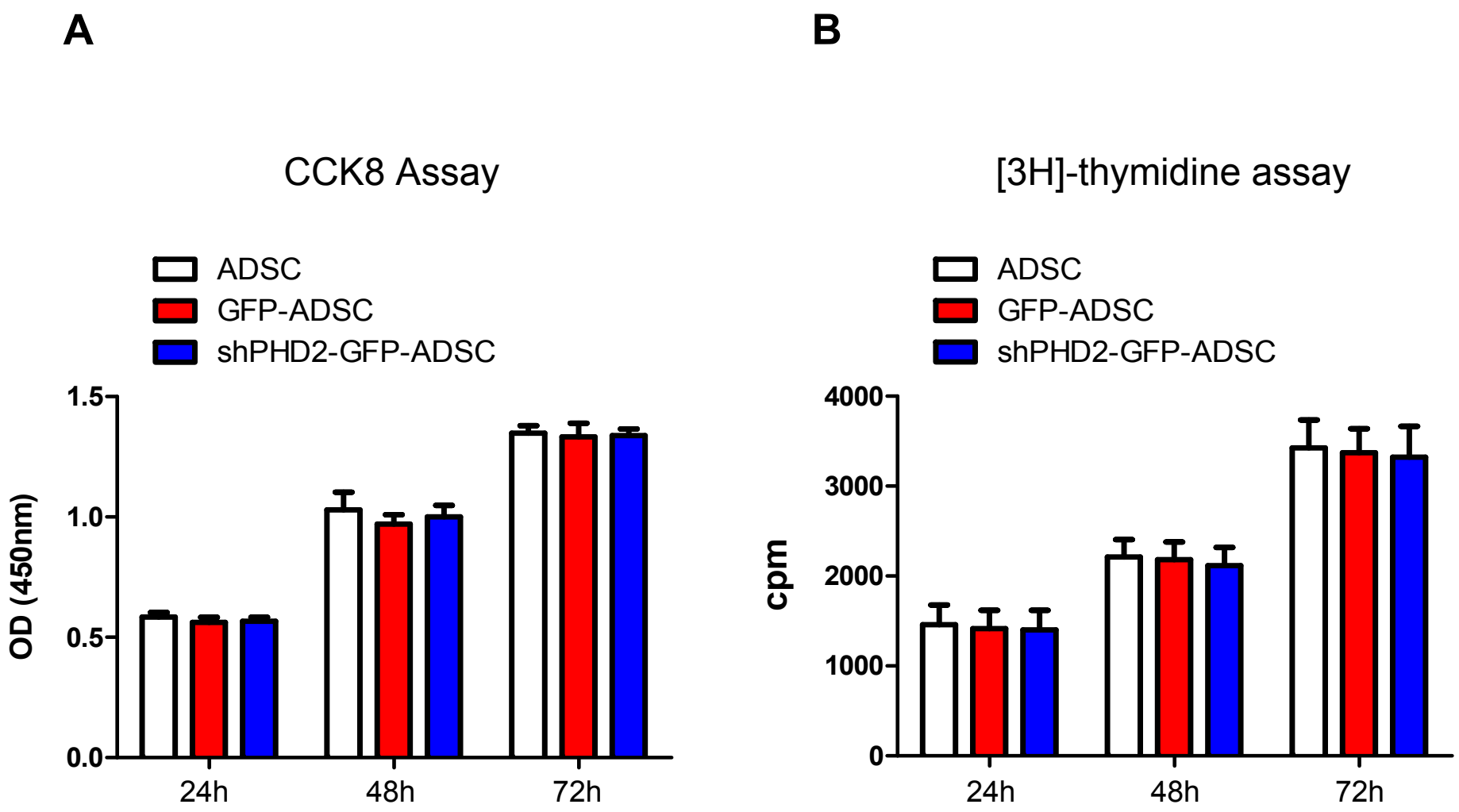

Online Figure VI

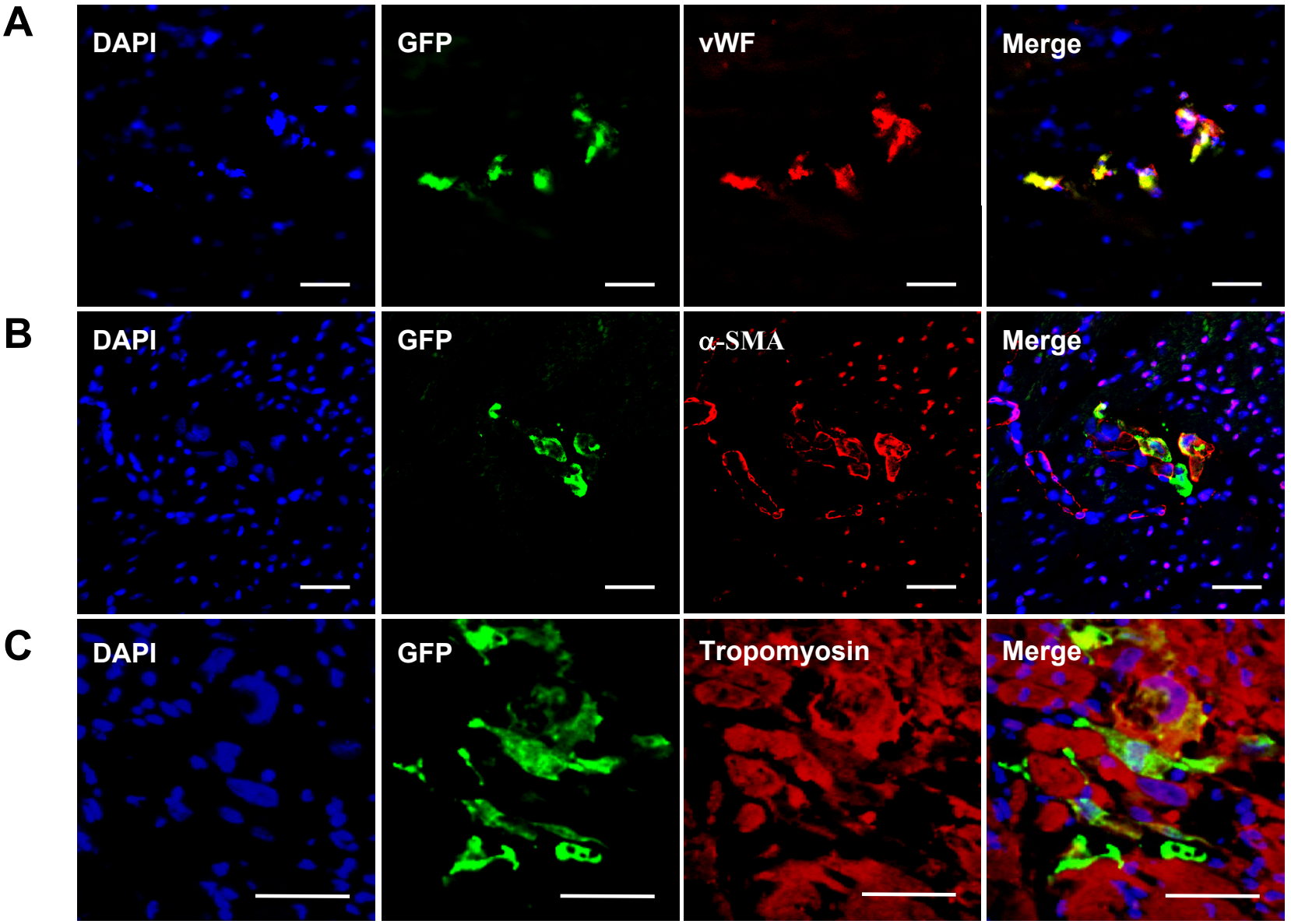

Online Figure VII

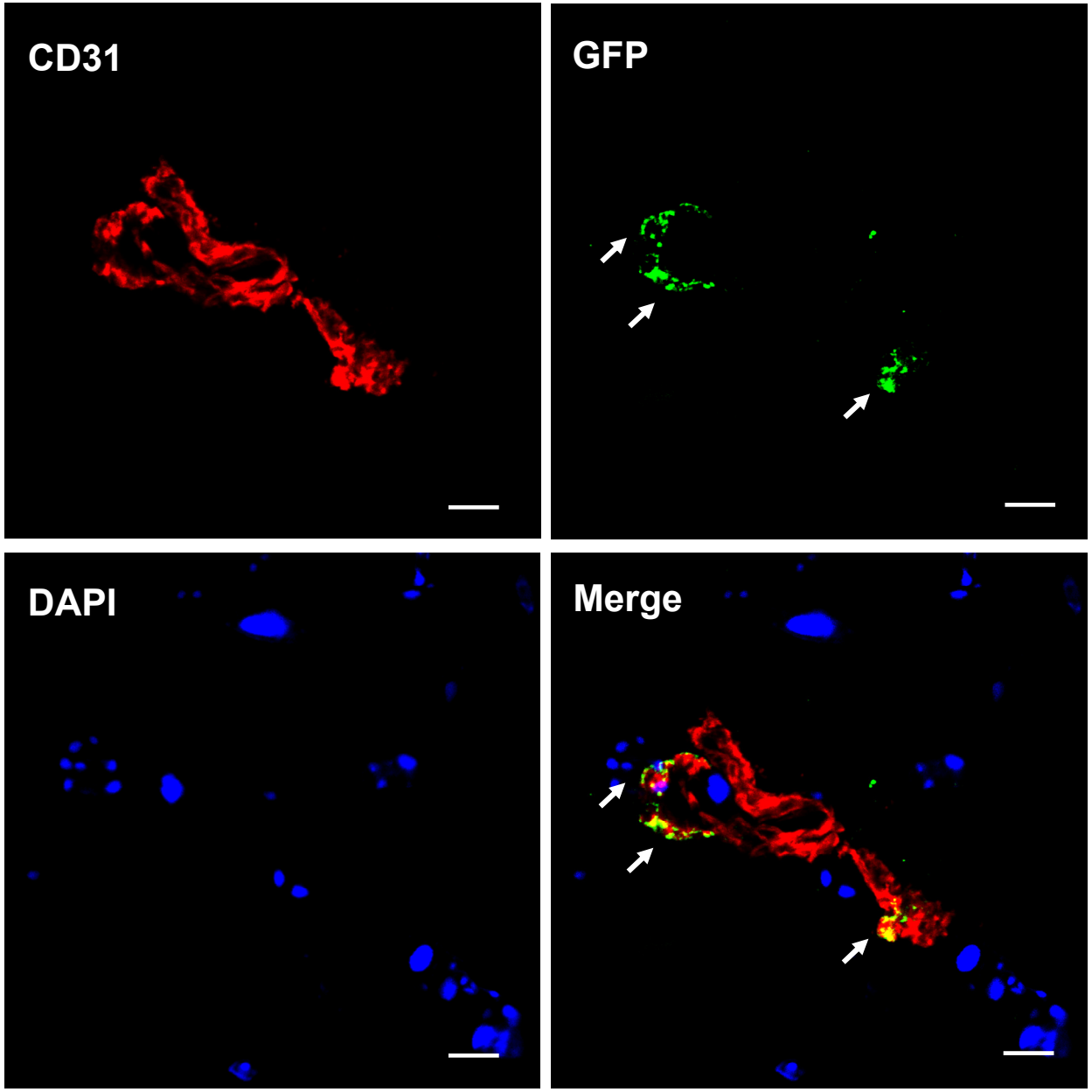

Online Figure VIII

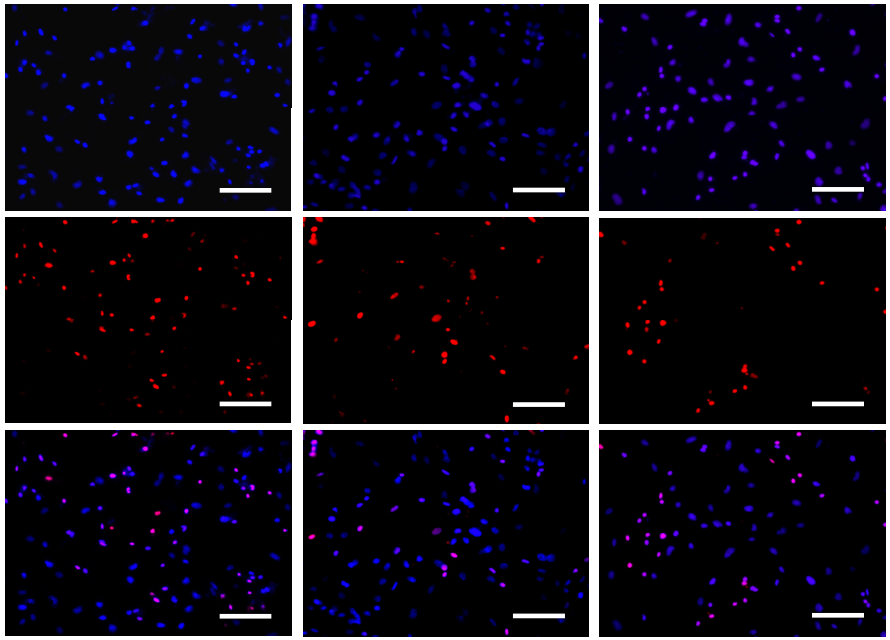

GFP-ADSC-CM	+	-	-
shPHD2-GFP-ADSC-CM	-	+	-
shHIF-1α/shPHD2-GFP-ADSC-CM	-	-	+
H_2O_2	+	+	+

Online Figure IX

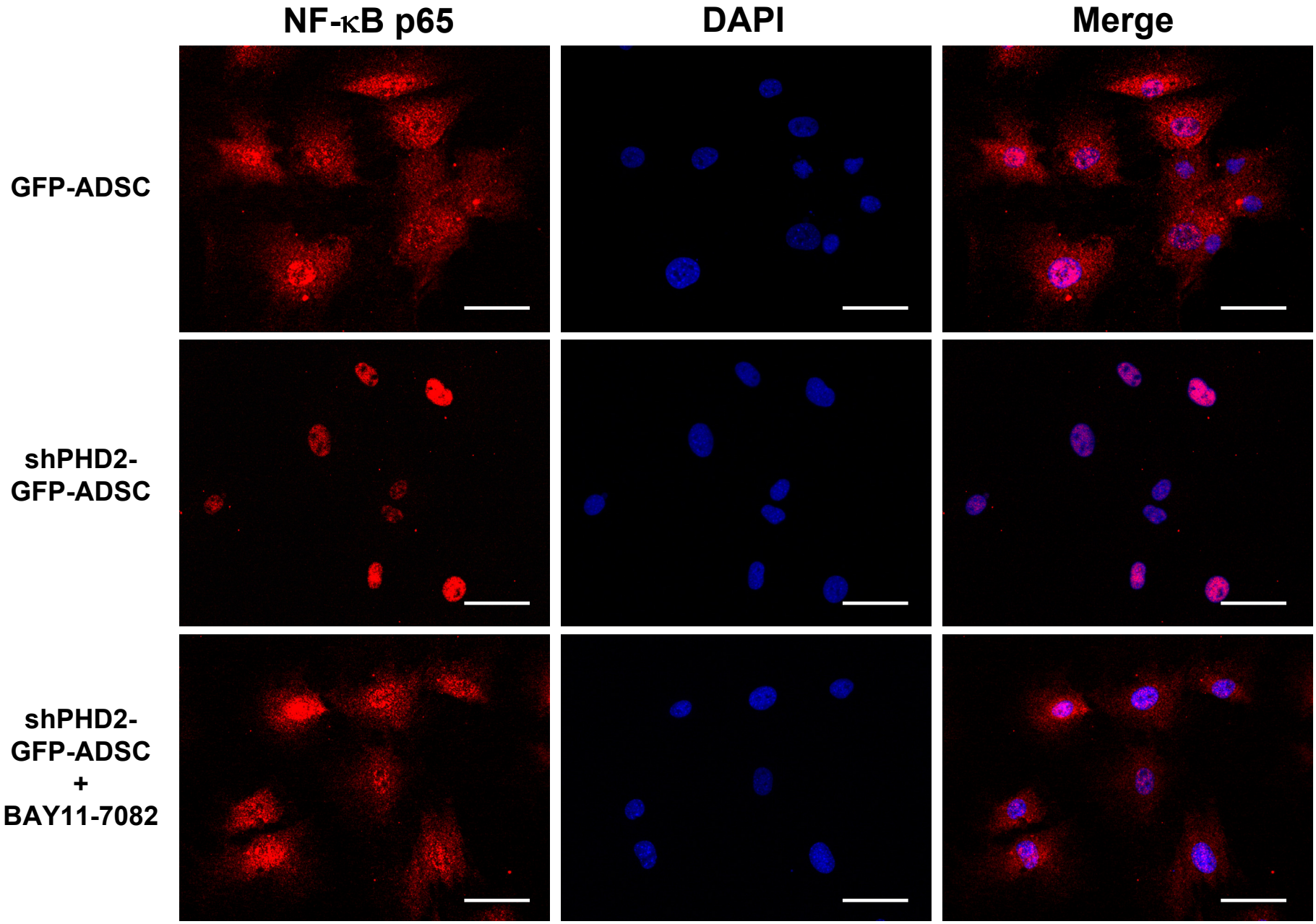

Online Figure X

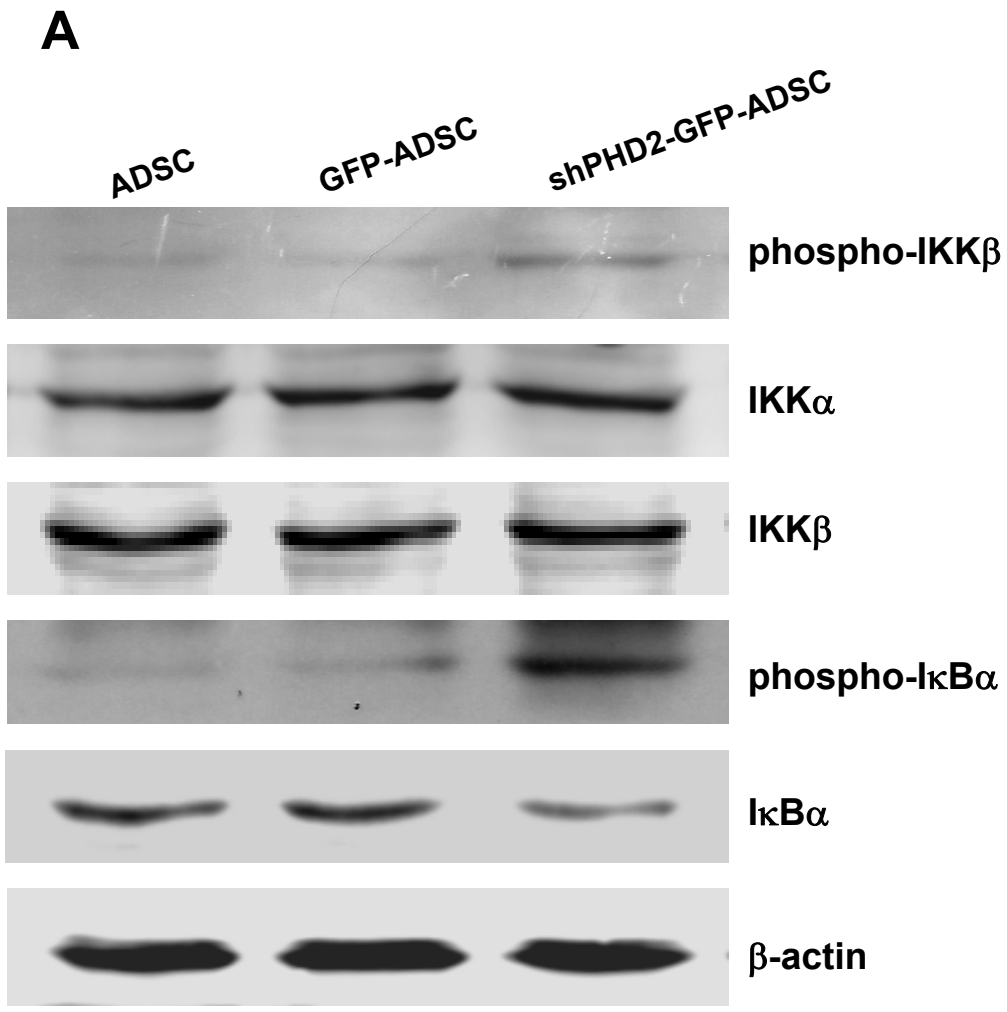

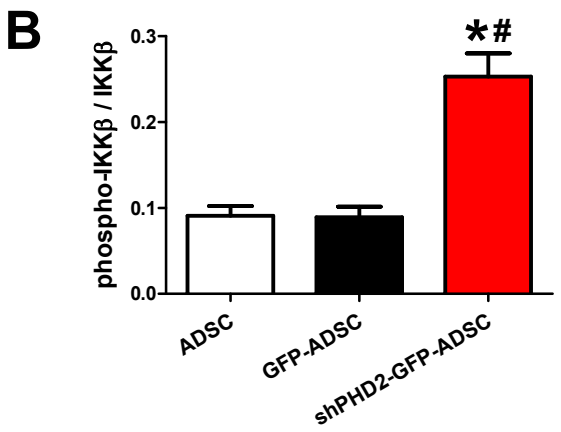

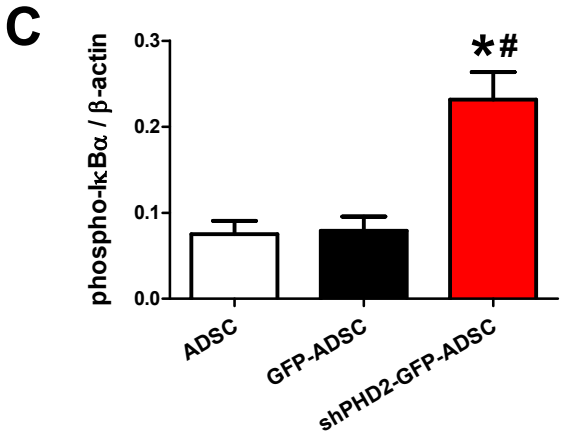

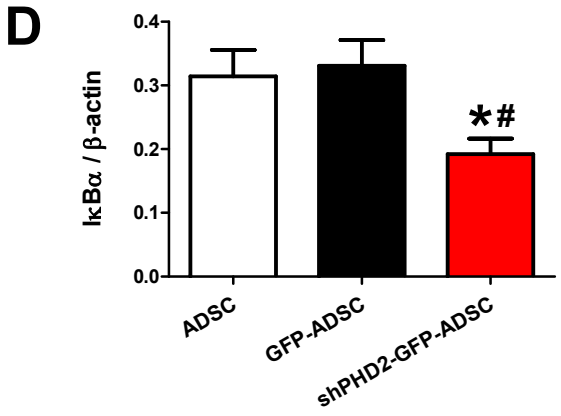

Online Figure XI

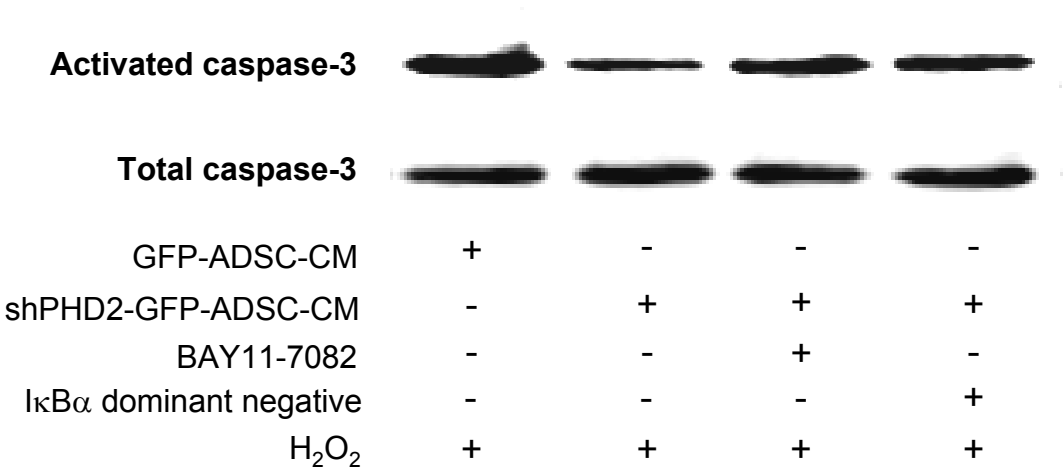

Online Figure XII

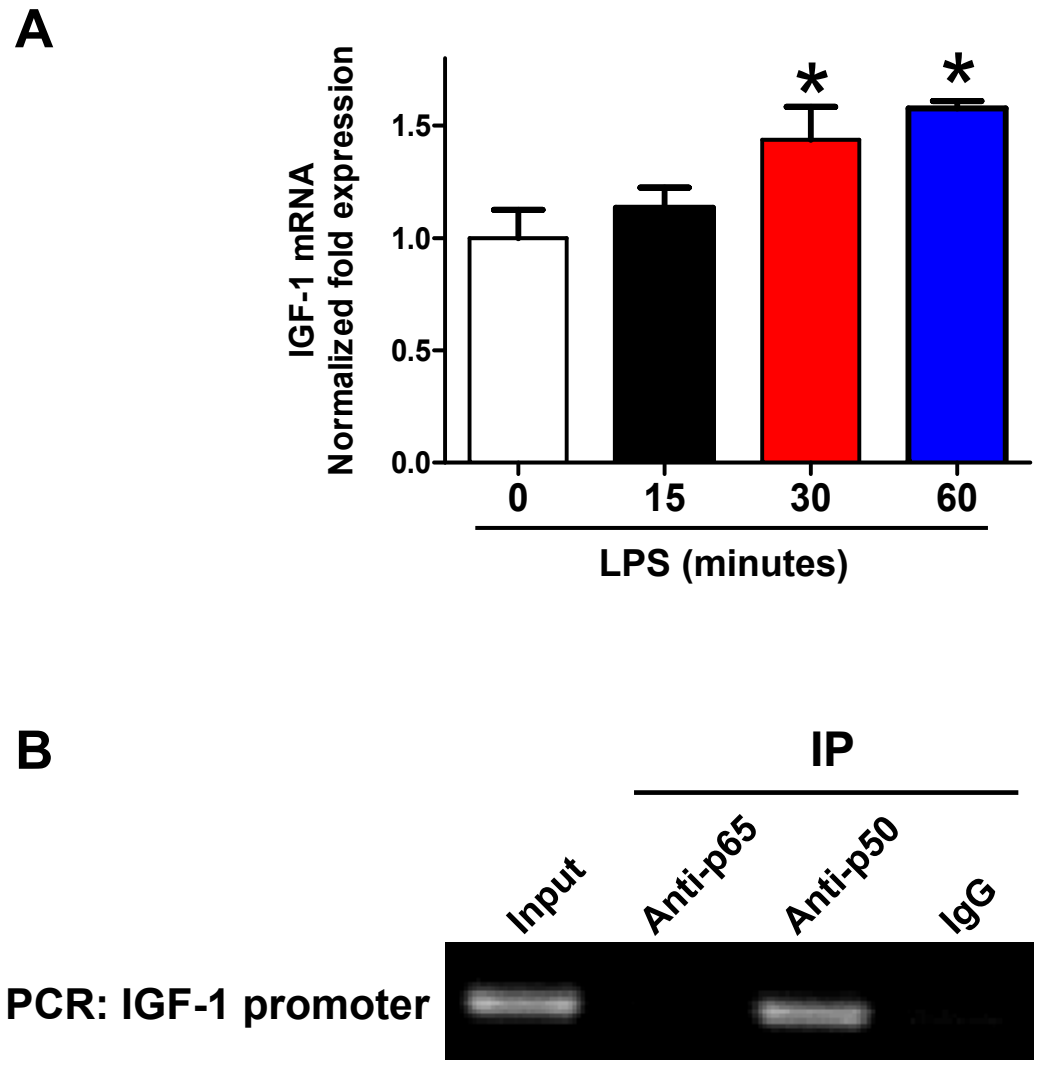

Online Figure XIII

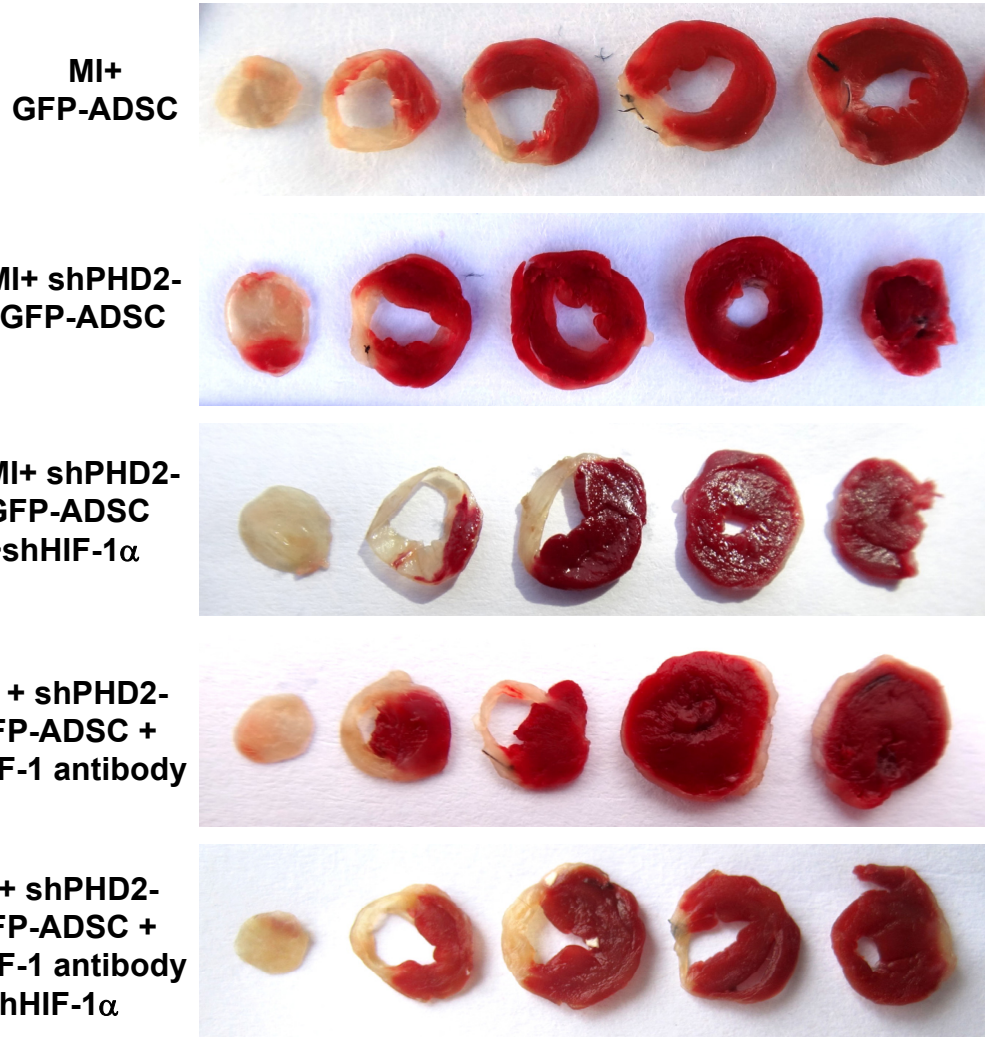

Online Figure XIV

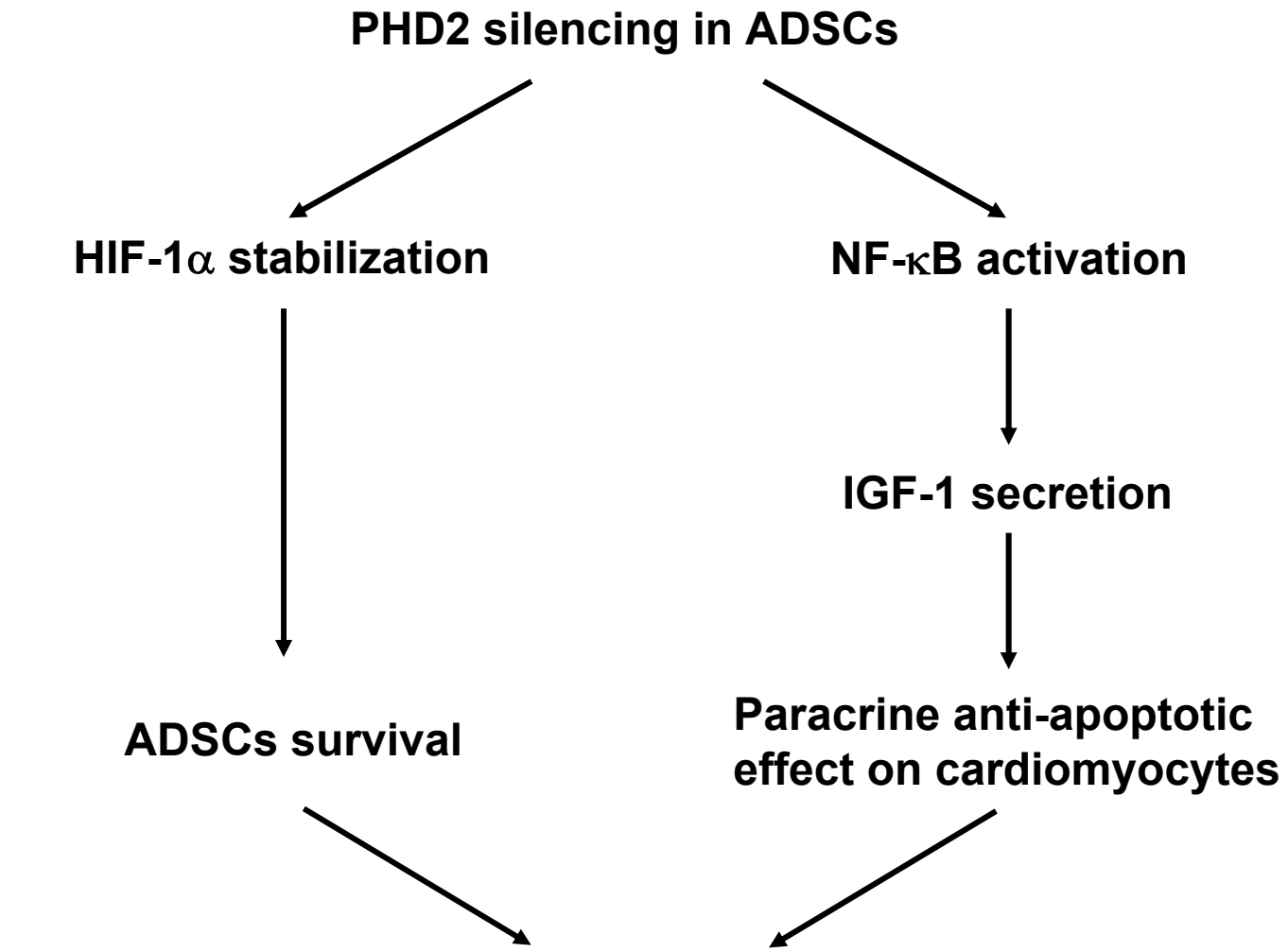

Online Table I

	Average Induction	Array #1			Array #2		
		GFP-ADSC	shPHD2-GFP-ADSC	x-fold	GFP-ADSC	shPHD2-GFP-ADSC	x-fold
IGF-I	**3.81**	0.1115	0.0338	3.30	0.4565	0.1057	4.32
Thrombopoietin	**2.83**	0.3043	0.1221	2.49	0.0836	0.0264	3.17
Osteoprotegerin	**2.63**	0.5431	0.2545	2.13	0.9121	0.2914	3.13
GM-CSF	**2.49**	0.0873	0.0481	1.82	0.1179	0.0372	3.16
BLC	**1.97**	0.2274	0.1365	1.67	0.3002	0.1322	2.27
TGF-β 3	**1.61**	0.2459	0.1609	1.53	0.4177	0.247	1.69
IL-16	**1.58**	0.3975	0.2893	1.37	0.6094	0.3396	1.79
IGFBP-1	**1.46**	0.4703	0.3381	1.39	1.0488	0.6877	1.53
EGF	**1.43**	0.2315	0.1727	1.34	0.3601	0.2376	1.52

Online Table II

	Average Induction	Array #1			Array #2		
		GFP-ADSC	shPHD2-GFP-ADSC	x-fold	GFP-ADSC	shPHD2-GFP-ADSC	x-fold
IL-8	**1.29**	0.2898	0.2178	1.33	0.3214	0.2578	1.25
IL-10	**1.26**	0.1137	0.0972	1.17	0.2097	0.1544	1.36
IL-1β	**1.23**	0.2556	0.2162	1.18	0.3764	0.2932	1.28
TNF-α	**1.22**	0.4614	0.3373	1.37	0.7833	0.7353	1.07
CCL-5	**1.18**	0.2526	0.2063	1.22	0.7653	0.6720	1.14
IL-2	**1.14**	0.1231	0.0923	1.33	0.1864	0.1969	0.95
GCP-2	**1.14**	0.2961	0.2523	1.17	0.4246	0.3843	1.10
IGFBP-2	**1.13**	0.4403	0.3384	1.30	0.5083	0.5284	0.96
IL-1α	**1.11**	0.3360	0.3478	0.97	0.5743	0.4567	1.26
MIP-3α	**1.10**	0.0744	0.0609	1.22	0.2179	0.2236	0.97
IL-15	**1.08**	0.1047	0.1169	0.90	0.1387	0.1099	1.26
MCP-1	**1.06**	0.2144	0.1841	1.16	0. 3406	0.3594	0.95
TNF-β	**1.02**	0.3432	0.3871	0.88	0.7275	0.6326	1.15
MIG	**0.95**	0.0737	0.0879	0.84	0.1543	0.1454	1.06
IL-12	**0.92**	0.2186	0.2109	1.04	0.3444	0.4279	0.80
MIP-1β	**0.89**	0.4719	0.5870	0.80	0.9599	0.9931	0.97
IL-13	**0.82**	0.0242	0.0317	0.76	0.0422	0.0481	0.88

Online Figure and Table Legends

Online Figure I. Characterization of human ADSCs. A: Lipogenenic and osteogenic differentiation of ADSCs were determined by histochemical staining of adipocytes (oil red O, left panel) and osteocytes (Alizarin red, right panel). Scale bar = 100 μm. B: Flow cytometric analysis shows that ADSCs were positive for CD90, CD73, CD44 and CD105 and negative for CD34 and CD45. ADSC: adipose-derived stem cell.

Online Figure II. Representative figures of $TUNEL^+$ cardiomyocytes in infarct border zone at 2 days after PBS or GFP-ADSCs or shPHD2-GFP-ADSCs injection. $TUNEL^+$ nuclei are stained green, tropomyosin is red and DAPI is blue. Scale bar = 50 μm.

Online Figure III. Representative images at low magnification and expanded view of the peri-infarct zone of hearts with Masson's trichrome staining at 4 weeks post-MI.

Online Figure IV. Effect of shPHD2-ADSC treatment on neutrophil and monocyte infiltration in infracted heart. Mice subjected to MI injury were injected with PBS, GFP-ADSCs, or shPHD2-GFP-ADSCs. Inflammatory cell populations in hearts at 2 days after transplantation were analyzed by FACS. Representative FACS plots show myeloid cells in the heart, defined by expression of CD45 and CD11b. The live-cell gate is shown on the left (forward vs. side scatter). Gating on myeloid cells ($CD11b^+/CD45^+$), infiltrated monocytes were defined ($Ly6C^{high}/Ly6G^-$). Corresponding percentages of each population are depicted by the bar graph at the right (N=6).* $p<0.05$ vs. Sham; # $p<0.05$ vs. MI+PBS.

Online Figure V. Effect of PHD2 silencing on ADSC proliferation. CCK-8 assay (A) and [3H]-thymidine assay (B) were performed in ADSCs at indicated time points. N=5.

Online Figure VI. Immunofluorescence analysis of ADSC differentiation at 4 weeks after transplantation. Sections of hearts intramyocardially injected with ADSCs were triple-stained with DAPI (nuclei), antibodies to GFP (for tracking ADSCs), and a third antibody against von Willebrand factor (endothelial cell marker, panel A), smooth muscle actin (SMA, smooth muscle cell marker, panel B), or sarcomeric tropomyosin (cardiomyocyte marker, panel C) as indicated. Scale bar = 25 μm. DAPI: 4′,6-diamidino-2-phenylindole.

Online Figure VII. Representative figures of immunostaining GFP, CD31 and DAPI in the infarcted hearts at 4 weeks after ADSC transplantation. Arrows indicate $GFP^+/CD31^+$ cells in heart vasculature, suggesting newly incorporated cells derived from transplanted ADSCs into blood vessels. Scale bar = 5 μm.

Online Figure VIII. Representative images of TUNEL staining in cardiomyocytes (quantification shown in Figure 7I). Cell nuclei were stained with DAPI (blue) and $TUNEL^+$ nuclei were stained with TMR-red.

Online Figure IX. Effect of PHD2 silencing on nuclear translocation of NF-κB in ADSCs. The intracellular location of NF-κB p65 in ADSCs was determined by immunofluorescence. shPHD2-ADSCs were treated with or without NF-κB inhibitor BAY11-7082. Cell nuclei were stained with DAPI (blue) and NF-κB p65 was stained in red. Scale bar = 50 μm.

Online Figure X. The regulation of PHD2 silencing on NF-κB signaling in ADSCs. A: Representative blots for phospho-IKKβ, total IKKα, total IKKβ, phospho-IκBα and total IκBα in ADSCs with or without PHD2 silencing. β-actin is used as control. B-D: Quantification of phospho-IKKβ/total IKKβ (B), phospho-IκBα/β-actin (C) and IκBα/β-actin (D). N=4. *$p<0.05$ vs. ADSCs; # $p<0.05$ vs. GFP-ADSCs.

Downloaded from http://circres.ahajournals.org/ at Temple University--Philadelphia on June 11, 2013

Online Figure XI. Representative figures of Western blotting analysis of activated caspase-3 expression of NRVMs cultured with or without NF-κB inhibition (quantification shown in Figure 7L).

Online Figure XII. The regulation of NF-κB on IGF-1. A: Quantification of IGF-1 mRNA expression by qPCR in ADSCs treated with NF-κB stimulator lipopolysaccharide (LPS, 1μg/ml) at indicated time points. B: The p50 bound to the κB site within the IGF-1 promoter detected by ChIP assay. ADSCs were stimulated with NF-κB stimulator LPS (1μg/ml for 30min). ChIP analysis was performed using anti-p65, anti-p50, or control IgG antibodies for immunoprecipitation followed by PCR using primers for the specific IGF-1 promoter region in which the predicted NF-κB site is located. The PCR products were subjected to electrophoresis on 2% agarose gel. These results are representative of 3 independent experiments.

Online Figure XIII. Representative images of TTC-stained heart sections at 4 weeks after transplantation (quantification shown in Figure 8C).

Online Figure XIV. Hypothesized mechanisms for the therapeutic effect of transplantation of ADSCs with PHD2 silencing on infarcted myocardium.

Online Table I. Secreted factors induced by silencing of PHD2 in ADSCs. Antibody arrays detecting 79 secreted factors were incubated with conditioned medium collected from GFP-ADSCs and shPHD2-GFP-ADSCs. Data from two independent experiments are shown. Nine secreted factors were induced by >1.3-fold by silencing of PHD2 in both experiments, and are listed here according to their average induction by shPHD2-GFP-ADSCs versus GFP-ADSCs. IGF-1: insulin-like growth factor 1; GM-CSF: granulocyte-macrophage colony-stimulating factor; TGF-β3: transforming growth factor-β3; IL-16: Interleukin 16; IGFBP-1: IGF binding protein-1; EGF: epidermal growth factor.

Online Table II. The secretion of chemokines regulated by NF-κB downstream induced by silencing of PHD2 in ADSCs. Antibody arrays detecting 79 secreted factors were incubated with conditioned medium collected from GFP-ADSCs and shPHD2-GFP-ADSCs. Data from two independent experiments are shown. 17 NF-κB downstream proteins were induced <1.3-fold by silencing of PHD2, and are listed here according to their average induction by shPHD2-GFP-ADSCs versus GFP-ADSCs. TNF-α: Tumor necrosis factor-α; MIG: interferon-γ; MIP: macrophage inflammatory protein; MCP: monocyte chemoattractant protein; GCP: granulocyte chemotactic protein; CCL-5: chemokine (C-C motif) ligand 5.

Downloaded from http://circres.ahajournals.org/ at Temple University--Philadelphia on June 11, 2013

Supplemental References

1. Bai X, Yan Y, Song YH, Seidensticker M, Rabinovich B, Metzele R, Bankson JA, Vykoukal D, Alt E. Both cultured and freshly isolated adipose tissue-derived stem cells enhance cardiac function after acute myocardial infarction. *Eur Heart J*. 2010;31:489-501.
2. Kubo H, Jaleel N, Kumarapeli A, Berretta RM, Bratinov G, Shan X, Wang H, Houser SR, Margulies KB. Increased cardiac myocyte progenitors in failing human hearts. *Circulation*. 2008;118:649-657.
3. Li X, Yu X, Lin Q, Deng C, Shan Z, Yang M, Lin S. Bone marrow mesenchymal stem cells differentiate into functional cardiac phenotypes by cardiac microenvironment. *J Mol Cell Cardiol*. 2007;42:295-303.
4. Li Y, Hiroi Y, Ngoy S, Okamoto R, Noma K, Wang CY, Wang HW, Zhou Q, Radtke F, Liao R, Liao JK. Notch1 in bone marrow-derived cells mediates cardiac repair after myocardial infarction. *Circulation*. 2011;123:866-876.
5. Arnalich-Montiel F, Pastor S, Blazquez-Martinez A, Fernandez-Delgado J, Nistal M, Alio JL, De Miguel MP. Adipose-derived stem cells are a source for cell therapy of the corneal stroma. *Stem Cells*. 2008;26:570-579.
6. Zhou Y, Yuan J, Zhou B, Lee AJ, Ghawji M, Jr., Yoo TJ. The therapeutic efficacy of human adipose tissue-derived mesenchymal stem cells on experimental autoimmune hearing loss in mice. *Immunology*. 2011;133:133-140.
7. Yuan SH, Martin J, Elia J, Flippin J, Paramban RI, Hefferan MP, Vidal JG, Mu Y, Killian RL, Israel MA, Emre N, Marsala S, Marsala M, Gage FH, Goldstein LS, Carson CT. Cell-surface marker signatures for the isolation of neural stem cells, glia and neurons derived from human pluripotent stem cells. *PLoS One*. 2011;6:e17540.
8. Zhang H, Chen X, Gao E, MacDonnell SM, Wang W, Kolpakov M, Nakayama H, Zhang X, Jaleel N, Harris DM, Li Y, Tang M, Berretta R, Leri A, Kajstura J, Sabri A, Koch WJ, Molkentin JD, Houser SR. Increasing cardiac contractility after myocardial infarction exacerbates cardiac injury and pump dysfunction. *Circ Res*. 2010;107:800-809.
9. Xiong D, Heyman NS, Airey J, Zhang M, Singer CA, Rawat S, Ye L, Evans R, Burkin DJ, Tian H, McCloskey DT, Valencik M, Britton FC, Duan D, Hume JR. Cardiac-specific, inducible clc-3 gene deletion eliminates native volume-sensitive chloride channels and produces myocardial hypertrophy in adult mice. *J Mol Cell Cardiol*. 2010;48:211-219.
10. Son NH, Yu S, Tuinei J, Arai K, Hamai H, Homma S, Shulman GI, Abel ED, Goldberg IJ. Ppargamma-induced cardiolipotoxicity in mice is ameliorated by pparalpha deficiency despite increases in fatty acid oxidation. *J Clin Invest*. 2010;120:3443-3454.
11. Wang X, Jameel MN, Li Q, Mansoor A, Qiang X, Swingen C, Panetta C, Zhang J. Stem cells for myocardial repair with use of a transarterial catheter. *Circulation*. 2009;120:S238-246.
12. Angert D, Berretta RM, Kubo H, Zhang H, Chen X, Wang W, Ogorek B, Barbe M, Houser SR. Repair of the injured adult heart involves new myocytes potentially derived from resident cardiac stem cells. *Circ Res*. 2011;108:1226-1237.
13. Zhao T, Yang L, Sun Q, Arguello M, Ballard DW, Hiscott J, Lin R. The nemo adaptor bridges the nuclear factor-kappab and interferon regulatory factor signaling pathways. *Nat Immunol*. 2007;8:592-600.
14. van Poll D, Parekkadan B, Cho CH, Berthiaume F, Nahmias Y, Tilles AW, Yarmush ML. Mesenchymal stem cell-derived molecules directly modulate hepatocellular death and regeneration in vitro and in vivo. *Hepatology*. 2008;47:1634-1643.
15. Gnecchi M, He H, Noiseux N, Liang OD, Zhang L, Morello F, Mu H, Melo LG, Pratt RE, Ingwall JS, Dzau VJ. Evidence supporting paracrine hypothesis for akt-modified mesenchymal stem cell-mediated cardiac protection and functional improvement. *FASEB J*. 2006;20:661-669.
16. Gringhuis SI, den Dunnen J, Litjens M, van Het Hof B, van Kooyk Y, Geijtenbeek TB. C-type lectin dc-sign modulates toll-like receptor signaling via raf-1 kinase-dependent acetylation of

Downloaded from http://circres.ahajournals.org/ at Temple University--Philadelphia on June 11, 2013

transcription factor nf-kappab. *Immunity*. 2007;26:605-616.
17. Vegran F, Boidot R, Michiels C, Sonveaux P, Feron O. Lactate influx through the endothelial cell monocarboxylate transporter mct1 supports an nf-kappab/il-8 pathway that drives tumor angiogenesis. *Cancer Res*. 2011;71:2550-2560.
18. Zhang H, Zhi L, Moochhala S, Moore PK, Bhatia M. Hydrogen sulfide acts as an inflammatory mediator in cecal ligation and puncture-induced sepsis in mice by upregulating the production of cytokines and chemokines via nf-kappab. *Am J Physiol Lung Cell Mol Physiol*. 2007;292:L960-971.
19. Shen Z, Peedikayil J, Olson GK, Siebert PD, Fang Y. Multiple transcription factor profiling by enzyme-linked immunoassay. *Biotechniques*. 2002;32:1168, 1170-1162.
20. Eyler CE, Wu Q, Yan K, MacSwords JM, Chandler-Militello D, Misuraca KL, Lathia JD, Forrester MT, Lee J, Stamler JS, Goldman SA, Bredel M, McLendon RE, Sloan AE, Hjelmeland AB, Rich JN. Glioma stem cell proliferation and tumor growth are promoted by nitric oxide synthase-2. *Cell*. 2011;146:53-66.
21. Ding J, Huang S, Wu S, Zhao Y, Liang L, Yan M, Ge C, Yao J, Chen T, Wan D, Wang H, Gu J, Yao M, Li J, Tu H, He X. Gain of mir-151 on chromosome 8q24.3 facilitates tumour cell migration and spreading through downregulating rhogdia. *Nat Cell Biol*. 2010;12:390-399.

Downloaded from http://circres.ahajournals.org/ at Temple University--Philadelphia on June 11, 2013